

Connectometry: A statistical approach harnessing the analytical potential of the local connectome



Fang-Cheng Yeh ^{a,*}, David Badre ^b, Timothy Verstynen ^{a,*}

^a Department of Psychology, Carnegie Mellon University, PA, USA

^b Department of Cognitive, Linguistic and Psychological Sciences, Brown University, RI, USA

ARTICLE INFO

Article history:

Received 18 August 2015

Accepted 19 October 2015

Available online 21 October 2015

Keywords:

Connectome

Connectometry

Diffusion MRI

Diffusion spectrum imaging

q-Space diffeomorphic reconstruction

Generalized q-sampling imaging

Quantitative anisotropy

ABSTRACT

Here we introduce the concept of the local connectome: the degree of connectivity between adjacent voxels within a white matter fascicle defined by the density of the diffusing spins. While most human structural connectomic analyses can be summarized as finding global connectivity patterns at either end of anatomical pathways, the analysis of local connectomes, termed connectometry, tracks the local connectivity patterns along the fiber pathways themselves in order to identify the subcomponents of the pathways that express significant associations with a study variable. This bottom-up analytical approach is made possible by reconstructing diffusion MRI data into a common stereotaxic space that allows for associating local connectomes across subjects. The substantial associations can then be tracked along the white matter pathways, and statistical inference is obtained using permutation tests on the length of coherent associations and corrected for multiple comparisons. Using two separate samples, with different acquisition parameters, we show how connectometry can capture variability within core white matter pathways in a statistically efficient manner and extract meaningful variability from white matter pathways, complements graph-theoretic connectomic measures, and is more sensitive than region-of-interest approaches.

© 2015 Elsevier Inc. All rights reserved.

Introduction

The human connectome refers to the map of connections between distinct cortical regions (Akil et al., 2011; DeFelipe, 2010; Seung, 2011; Turk-Browne, 2013), where connectivity is typically quantified using functional (e.g., functional MRI, electrophysiological approaches) (Biswal et al., 2010; Dolgin, 2010; Fornito et al., 2015; Honey et al., 2009; Johansen-Berg et al., 2004) or structural measurements (e.g., diffusion MRI) (Craddock et al., 2013; Hagmann et al., 2010b; Pestilli et al., 2014; Wedeen et al., 2012). Diffusion MRI is currently the most popular method for measuring the structural connectome in humans. It allows for mapping macroscopic end-to-end connections between parcellated gray matter targets using a fiber tracking algorithm (Sporns, 2013; Wedeen et al., 2012), and the streamline count of the connections can be used as a measure of global connectivity in several connectomic studies (Fig. 1a) (Bullmore and Sporns, 2009; Hagmann et al., 2008; Hagmann et al., 2007; Hagmann et al., 2010b; Sporns, 2014a, b). These structural connectomic approaches have used connectivity matrices to represent the graph structure of connectome, and graph-theoretic measures were estimated from these matrices to

study how topological patterns varied along experiment-relevant dimensions. However, these “find-difference-in-track” approaches heavily rely on diffusion MRI tractography to quantify end-to-end connectivity. While diffusion MRI tractography has increased in popularity over the last decade, several recent studies have identified critical concerns with the reliability of end-to-end connectivity measurement (Reveley et al., 2015; Thomas et al., 2014). Specifically, fiber tracking algorithms have exhibited limited reliability near the gray matter targets, thus putting into question the reliability of these “find-difference-in-track” methods.

To bypass the limitations of end-to-end fiber tracking, we introduce the concept of the *local* connectome: the degree of connectivity between adjacent voxels within a white matter fascicle defined by the density of the diffusing spins (Fig. 1b). Since the entire connectome is defined as the complete map of connections in the brain, knowing the local orientation and integrity of the fiber bundles as they run through the core of white matter is just as important as knowing where a bundle starts and stops. In this way the local connectome can be viewed as the fundamental unit of the end-to-end structural connectome, and thus analyzing the local connectomes along fiber bundles may serve as a surrogate for the global end-to-end connectivity analysis. The mapping and analysis of local connectomes, termed connectometry, adopted a “track-difference” paradigm. Instead of mapping the entire end-to-end connectome, connectometry tracks only the segment of fiber bundle that exhibits significant association with the study variable. This is

* Corresponding authors at: Department of Psychology and Center for the Neural Basis of Computation, Carnegie Mellon University, Pittsburgh, PA, USA.

E-mail addresses: frank.yeh@gmail.com (F.-C. Yeh), [\(T. Verstynen\)](mailto:timothyv@andrew.cmu.edu).

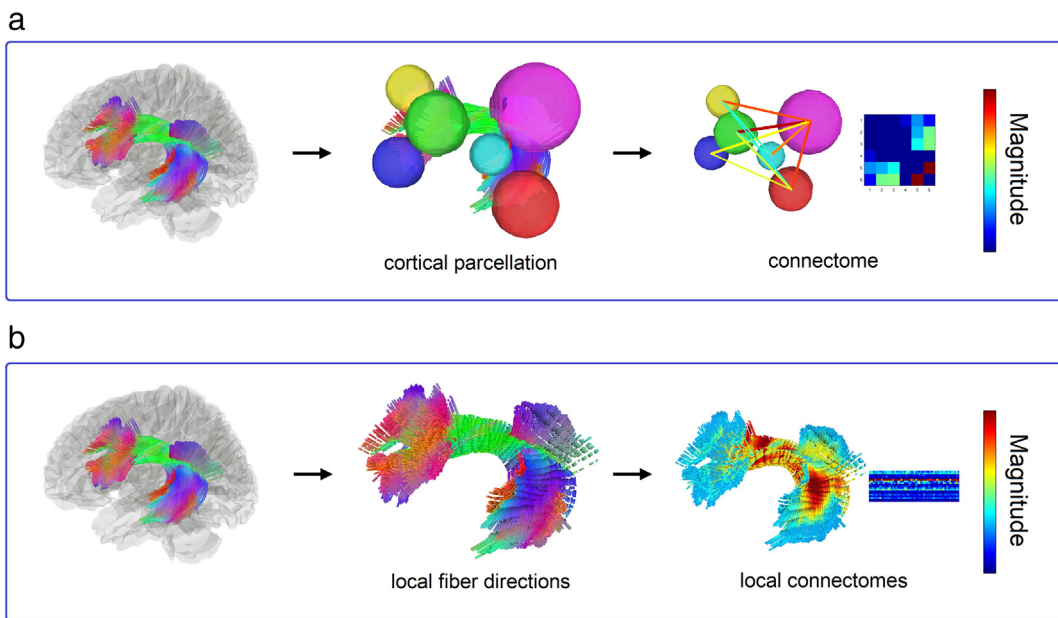


Fig. 1. Differences between the global connectome and local connectome. (a) The mapping of human connectome relies on cortical parcellation to define a set of common regions (nodes) for calculating the connectivity measurements (edges). The connectivity can be measured by the number of the connecting tracks or their mean anisotropy value. The final form can be expressed as a symmetric connectivity matrix. (b) The mapping of local connectome utilizes local fiber directions from a common atlas to sample the density of diffusing spins as the connectivity measurement. Multiple measurements can be obtained along the fiber pathways to reveal the change of track compactness within a fiber bundle. The local connectome of a subject can be represented by a row vector, whereas the local connectomes from a group of subjects can be compiled as a local connectome matrix.

realized by reconstructing diffusion MRI data into a standard template space to map a local connectome matrix from a group of subjects (Fig. 2a). Study-relevant variables are then associated with this local connectome matrix in order to identify local connectomes that express significant associations with the variable of interest (Fig. 2b). These local connectomes are then tracked along the core pathway of a fiber bundle using a fiber tracking algorithm and compared with a null distribution of coherent associations using permutation statistics (Nichols and Holmes, 2002) (Fig. 2c). Permutation testing allows for estimating and correcting the false discovery rate (FDR) of Type-I error inflation due to multiple comparisons. We show how different levels of FDR can be devised to tune the sensitivity and specificity of connectometry for exploratory purposes (high FDR) or confirmatory purposes (low FDR).

We benchmarked the performance of connectometry by replicating a well-established negative association between global white matter integrity and physical obesity (Gianaros et al., 2013; Mueller et al., 2011; Stanek et al., 2011; Verstynen et al., 2013, Verstynen et al., 2012). This was done using two data sets acquired in different imaging

environments and using two different forms of high angular resolution diffusion MRI. By comparing our results against traditional tractography and region-of-interest approaches, we show how connectometry can complement conventional end-to-end connectivity analyses and provide a more nuanced description of variability within core white matter pathways.

Methods

Diffusion MRI acquisitions

The first data sample consisting of a total of 60 subjects with no previous history of neurological or mental disorder were scanned on a Siemen's Verio 3 T system in the Scientific Imaging & Brain Research Center at Carnegie Mellon University (abbreviated as CMU hereafter) using a 32-channel head coil. We collected a 50 min, 257-direction diffusion spectrum imaging (DSI) scan using a twice-refocused spin-echo EPI sequence and multiple q values (TR = 9916 ms, TE = 157 ms,

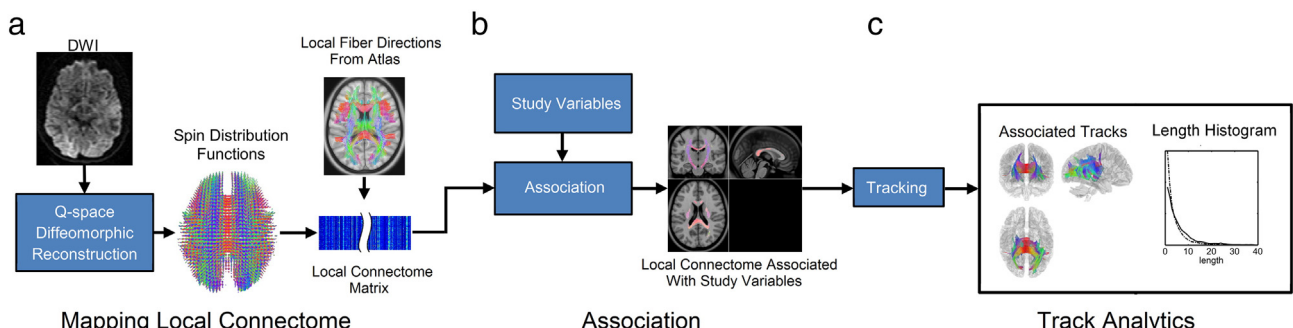


Fig. 2. Diagram of the connectometry pipeline. (a) The diffusion data of each subject are reconstructed in a common standard space, and the calculated spin distribution functions are then sampled by the local fiber directions from a common atlas to estimate the local connectome. The local connectome of a group of subjects can be compiled as a local connectome matrix. (b) The local connectome matrix is then associated with study variables using relevant statistical procedures (e.g., using a multiple regression model). (c) The local connectomes that express positive or negative association with the study variable can be tracked along a common pathway to reveal the subcomponents of the fascicles that have significant associations. The length histogram of these subcomponents is calculated, and the statistical inference can be obtained by comparing the findings with a null distribution to estimate the false discovery rate.

voxel size = $2.4 \times 2.4 \times 2.4$ mm, FoV = 231×231 mm, b-max = 5000 s/mm 2 , 51 slices). Head-movement was minimized during the image acquisition through padding supports and all subjects were confirmed to have minimal head movement during the scan prior to inclusion in the template. Another set of 20 subjects with no previous history of neurological or mental disorder was scanned in a Siemens 3 T Tim Trio System at Brown University (abbreviated as BU hereafter). A twice-refocused spin-echo sequence was used to acquire DSI with a 32-channel head coil. The total diffusion sampling direction was 257. The spatial resolution was 2.4 mm isotropic. TR = 9900 ms, and TE = 157 ms. The maximum b-value was 7000 s/mm 2 .

The second data set was from the Human Connectome Project consortium led by Washington University, University of Minnesota, and Oxford University (abbreviated as the WU-Minn HCP). 488 of subjects received diffusion MRI scans. The scan was acquired in a Siemens 3 T Skyra scanner using a 2D spin-echo single-shot multiband EPI sequence with a multi-band factor of 3 and monopolar gradient pulse (Sotiroopoulos et al., 2013). The spatial resolution was 1.25 mm isotropic. TR = 5500 ms, TE = 89.50 ms. The b-values were 1000, 2000, and 3000 s/mm 2 . The total number of diffusion sampling directions was 90, 90, and 90 for each of the shells in addition to 6 b0 images. The total scanning time was approximately 55 min.

Connectometry

The diagram of the connectometry method is shown in Fig. 2. As shown in this overview figure, the diffusion data of each subject are reconstructed in a standard space using q-space diffeomorphic reconstruction, and the density of diffusing spins is then sampled by the local fiber directions from a common atlas to estimate the local connectome and to construct a local connectome matrix (Fig. 2a). Then the local connectome matrix is associated with study variables using relevant statistical procedures (e.g., using a multiple regression model) (Fig. 2b). The local connectomes that express positive or negative association with the study variable can be tracked along a common pathway to reveal the subcomponents of the fascicles that have significant associations. The length histogram of these subcomponents is calculated, and the statistical inference can be obtained by comparing the findings with a null distribution to estimate the false discovery rate (Fig. 2c). Each step of the connectometry method is detailed in the following sections.

Q-space diffeomorphic reconstruction

We reconstructed multiple sets of dMRI data into the Montreal Neurological Institute (MNI) space using q-space diffeomorphic reconstruction (Yeh and Tseng, 2011) (QSDR). QSDR satisfied the conservation of diffusion spins after non-linear spatial transformation and could be applied to diffusion tensor imaging (DTI), DSI, or multishell data (Yeh and Tseng, 2011) to calculate a spin distribution function (SDF) (Yeh et al., 2010), $\Psi(\hat{\mathbf{u}})$, an orientation distribution function defined as the density of diffusing spins that have a displacement oriented at direction $\hat{\mathbf{u}}$ during the diffusion time (Yeh and Tseng, 2011):

$$\psi(\hat{\mathbf{u}}) = \left| J_\varphi \right| Z_0 \sum_i W_i(\varphi(\mathbf{r})) \operatorname{sinc} \left(\sigma \sqrt{6Db_i} \langle \hat{\mathbf{g}}_i, \frac{J_\varphi \hat{\mathbf{u}}}{\| J_\varphi \hat{\mathbf{u}} \|} \rangle \right) \quad (1)$$

where φ is a spatial mapping function that maps a template space coordinates \mathbf{r} to the subject's space. The mapping function was calculated using a non-linear registration between subject anisotropy map and the anisotropy map in the MNI space (Ashburner and Friston, 1999). J_φ is the Jacobian matrix of the mapping function, whereas $|J_\varphi|$ is the Jacobian determinant. $W_i(\varphi(\mathbf{r}))$ are the diffusion signals acquired at $\varphi(\mathbf{r})$. b_i is the b-value, and $\hat{\mathbf{g}}_i$ is the direction of the diffusion sensitization gradient. σ is the diffusion sampling ratio controlling the detection

range of the diffusing spins. D is the diffusivity of water, and Z_0 is the constant estimated by the diffusion signals of free water. 2 mm resolution was assigned as the output resolution of the QSDR reconstruction for CMU and Brown University diffusion data, whereas the HCP data were reconstructed to 1 mm resolution. The SDFs of 60 subjects from CMU and 20 subjects from Brown University were averaged to create the CMU/BU-80 multisite atlas. The SDFs of HCP data at WU-Minn were averaged to construct the HCP-488 atlas. The SDF was sampled at a total of 642 sampling directions defined by an 8-fold tessellated icosahedron, and the local maxima (peaks) can be determined using the neighboring relation of the sampling directions. The peak directions on the averaged SDFs defined the local fiber directions that were used to measure the local connectomes in each subject.

Local connectome matrix associated with study variables

For each voxel, the local fiber directions from a common diffusion MRI atlas provided the principle directions to sample the magnitudes of subject SDFs as the local connectome properties. The local connectomes of subjects were estimated by the density of anisotropic spins diffusing along the local fiber orientation (Fig. 3a):

$$\psi(\hat{a}) - iso(\psi) \quad (2)$$

where ψ is the SDF of the subject reconstructed by QSDR at a voxel, and \hat{a} is the local fiber direction provided by a common dMRI atlas, and $iso(\psi)$ is the isotropic diffusion of the SDF estimated by taking the minimum value of the SDF. The local connectomes of a subject were stretched into a row vector, and the vectors from a group of subjects were compiled into a single local connectome matrix (Fig. 3b). Each row of the matrix represents the local connectome of a subject, whereas each column corresponds to a common fiber direction from the atlas. The calculated local connectome matrix had a dimension of n -by- m , where n is the subject count and m is the total number of local connectome values.

A total of 59 CMU subjects had recorded body mass index (BMI) measures, and the local connectomes from these subjects were estimated using Eq. (2), where the local fiber directions were identified from the CMU/BU 80 atlas. The local connectomes of these subjects were compiled into a local connectome matrix, where each row of the matrix represented the local connectome of a subject, and each column corresponded to each local fiber direction in the CMU/BU 80 atlas. We correlated the local connectome matrix with BMI, age, and sex using the following regression model (Fig. 2b):

$$\mathbf{Y} = \mathbf{X}\mathbf{B} \quad (3)$$

where \mathbf{Y} is an n -by- m local connectome matrix. n is the number of subjects, and m is the total number of local fiber directions in the dMRI atlas. \mathbf{X} is an n -by-4 matrix, recording the BMI, age, and sex of each subject, and additional column is an all 1 vector for intercept. \mathbf{B} is a 4-by- m coefficient matrix. Since $m > n$, \mathbf{B} can be calculated by a simple ordinary least square, $(\mathbf{X}^T \mathbf{X})^{-1} \mathbf{X}^T \mathbf{Y}$, and the first column of \mathbf{B} , denoted as β hereafter, is a vector of coefficients corresponding to BMI. Since the row vectors of \mathbf{X} and \mathbf{Y} are independent to others, the empirical distribution of \mathbf{B} can be obtained by applying 5000 bootstrap resampling to the row vectors of matrix \mathbf{X} . Similarly, the null distribution of \mathbf{B} can be obtained by applying 5000 random permutations to the row vectors.

Local connectomes and their statistical inference

The core hypothesis in connectometry is that the associations between local connectomes and the study variables tend to propagate along a common fiber pathway. This hypothesis can be tested by tracking local connectomes that express substantial association with BMI into a “track”, and comparing the length of this track with that from a

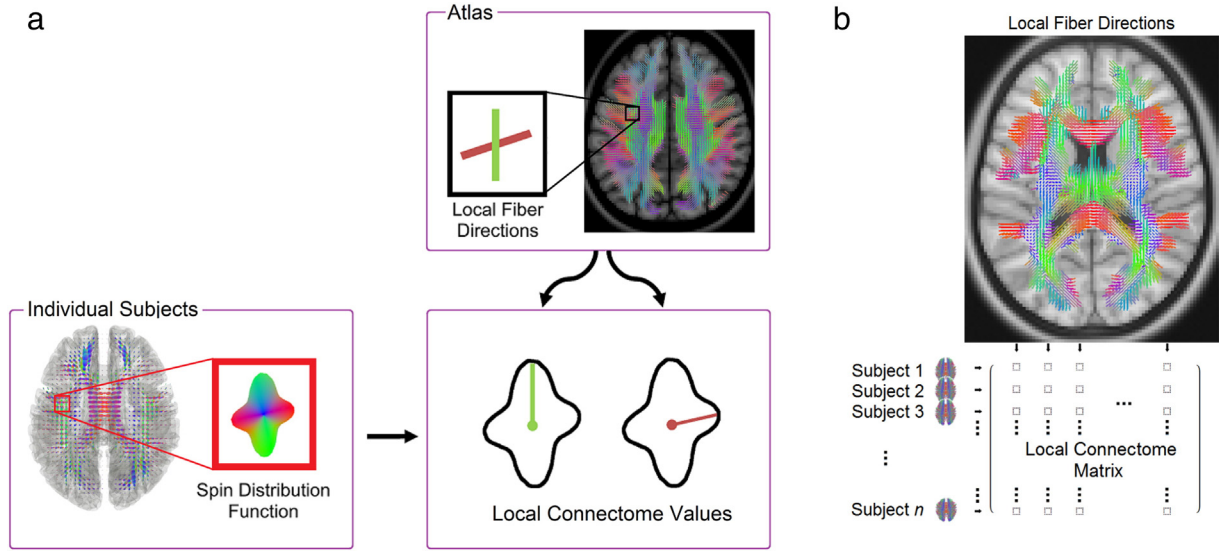


Fig. 3. (a) The magnitude of the spin distribution function at the fiber directions is used as the local connectome measurements. It is noteworthy that multiple fiber populations can coexist locally within a voxel, and each fiber population, identified by its fiber direction, has its unique local connectome estimation. (b) Compilation of a local connectome matrix from a group of subjects. The local connectomes of each subject are arranged as a row vector in the matrix, and the vectors of a group of subjects can be compiled as a matrix. Since the rows are independent to each other, a distribution of this local connectome matrix can be generated by applying bootstrapping to the row vectors. Similarly, a null distribution can also be generated by randomly permuting the row vectors.

null distribution (Fig. 4). The positive and negative associations were studied separately. To study negative associations, the local connectomes with coefficients of less than a predefined negative threshold were filtered in, whereas for positive associations, the local connectomes with a coefficient value greater than a predefined threshold were filtered in. The predefined thresholds were automatically determined using Otsu's threshold (Otsu, 1979). This association procedure identified local connectomes with substantial associations (colored sticks in Fig. 4), which may include true positive findings (red sticks) and false positive findings (blue sticks). The true positive findings (red sticks) could only be observed from the non-permuted local connectome matrix (lower row in Fig. 4), whereas the false positive findings could be observed from both non-permuted and permuted

matrices. This allowed us to model the null distribution by randomly permuting the local connectome matrix (upper row in Fig. 4). Using a tracking algorithm (Yeh et al., 2013b), we placed a total of 10 seeds per local connectome within its belonging voxel to start tracking. This tracking procedure was conducted for a set of 5000 local connectome matrices (without permutation) obtained from bootstrapping resampling and another *null* set of 5000 local connectome matrices obtained from random permutation. We formulated the null hypothesis for each track as: the length of a track connected along substantial coefficients in the non-permuted condition is not longer than that from the permuted condition. Since multiple tracks were connected throughout the brain space, we used false discovery rate to reject the null hypotheses and identified tracks with significant FDR. The length histograms of

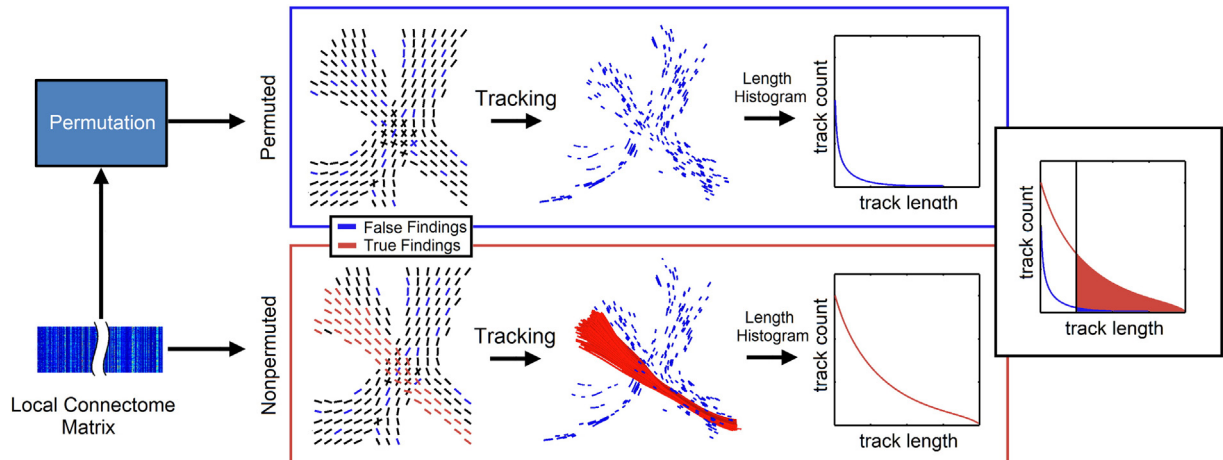


Fig. 4. Random permutation used to obtain the null distribution of the connectometry findings. The non-permuted local connectome matrix is regressed with the study variables (lower row), and the local connectomes that express associations can be visualized. The true findings (red sticks) tend to propagate along a common fiber pathway, whereas the false findings (blue sticks) are randomly distributed. The null distribution of the findings can be obtained by applying random permutation to the local connectome matrix (upper row). The permuted local connectome matrix is also regressed with the study variables to access the null distribution of the false findings (blue tracks). The tracks connected from false findings can be characterized by fragmented, short-ranged, tracks. By contrast, the true findings can be differentiated by its longer trajectories. Their difference can be quantified using a histogram of track length. We may view tracks with lengths greater than a threshold as true findings, and the false discovery rate can be calculated by the ratio of the area under the two distribution curves in the histogram.

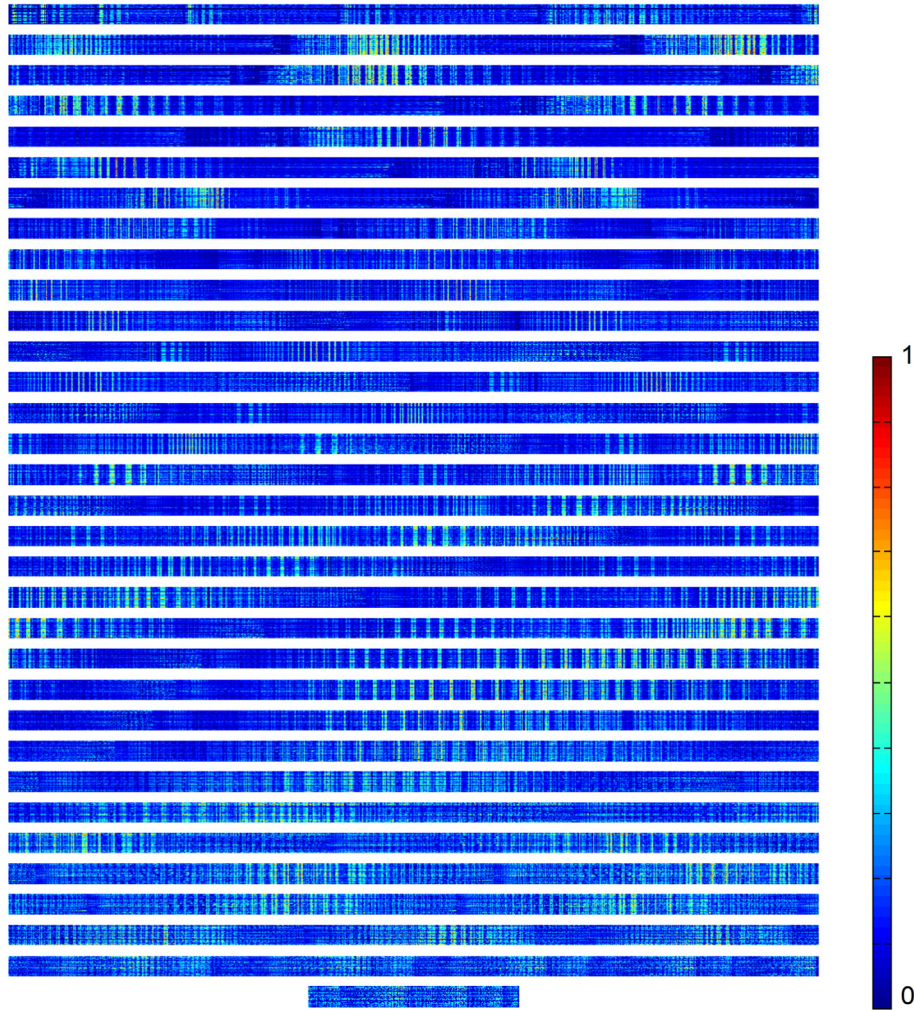


Fig. 5. The local connectome matrix of 59 subjects visualized. A local connectome matrix has a dimension of n -by- m , where n is the number of subjects, and m is the number of local connectome, around 80,000 at 2-mm resolution and 900,000 at 1-mm resolution. The figure shows the matrix divided in multiple rows to facilitate visualization.

the tracks were calculated, and the false discovery rate (FDR) of the tracks in non-permuted condition were calculated by the ratio of the area under the histogram curve.

In CMU 59 subjects' data, the FDR was controlled at 0.10, 0.075, and 0.05 to examine the results at different sensitivity/specificity levels. The same analysis was repeated on 488 subjects (all had BMI information) from the WU-Minn HCP Consortium to examine whether we could obtain consistent results from two independently acquired data sets.

Comparison with connectivity matrix

The 59 CMU subjects with BMI data were reconstructed using generalized q-sampling imaging (Yeh et al., 2010) with a length

ratio of 1.25. A total of 100,000 whole brain tracks were obtained using a fiber tracking algorithm (Yeh et al., 2013b). The default anisotropy threshold and step size (determined automatically in DSI Studio) were used. The angular threshold was 60° . The cortical parcellation was conducted by warping the subject space to a standard space using non-linear registration (Ashburner and Friston, 1999). The cortex was partitioned using the Automated Anatomical Labeling (AAL) atlas. A connectivity matrix was calculated for each subject, and the entry of the matrix was the mean quantitative anisotropy (QA) values of the corresponding tracks. The connectivity matrices of 59 subjects were regressed with their BMI, sex, and age using a linear regression model. The BMI-related coefficients and uncorrected p-value can be calculated for each matrix entry using a

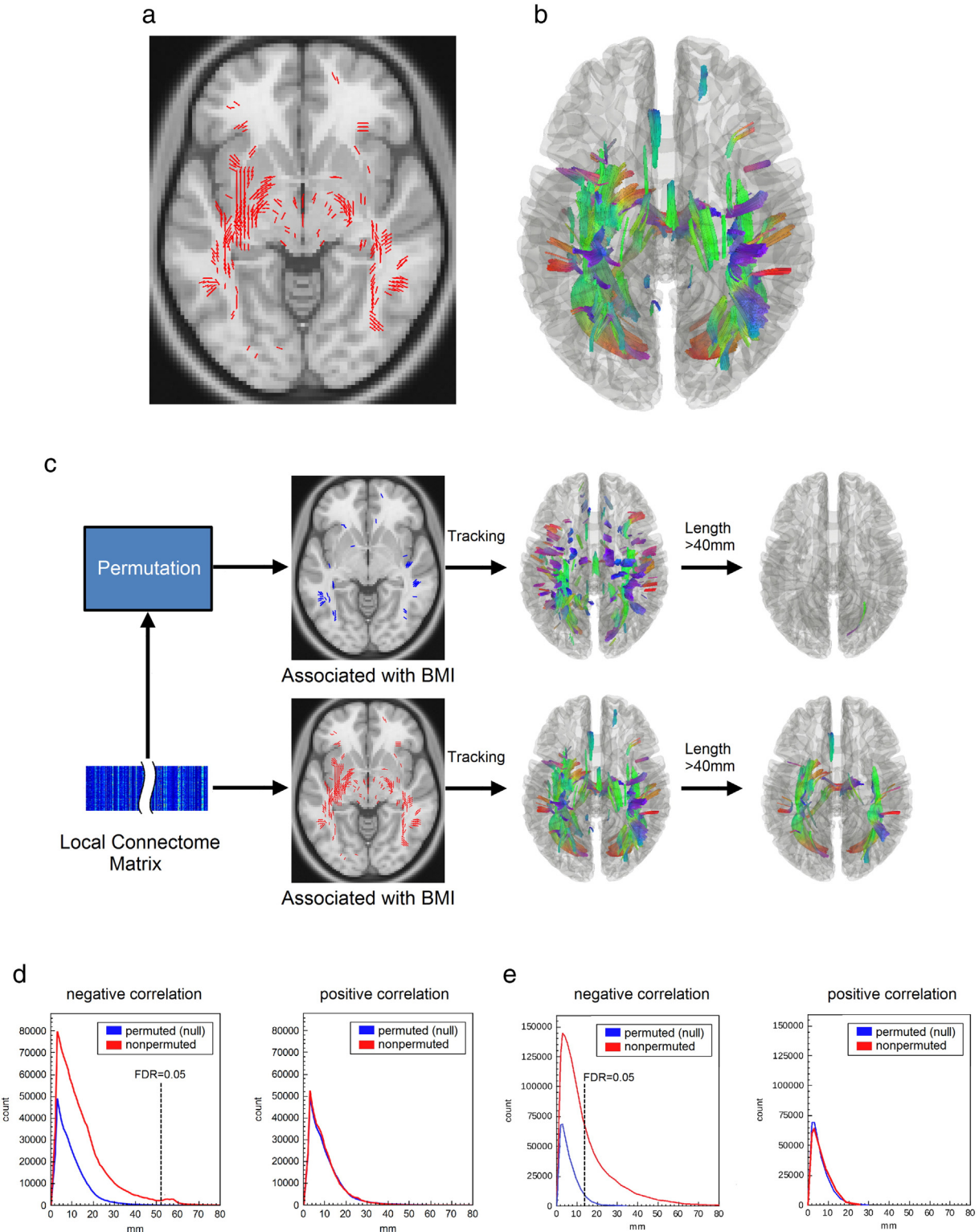
Fig. 6. The result of connectometry examined by a randomized permutation test. (a) The red sticks show local connectomes with substantial decrease of local connectome associated with high body mass index. The spatial distribution of these local connectomes follows the hypothesis that associations between local connectome patterns and study-relevant variables propagate along common fiber pathways. (b) A fiber tracking algorithm can be used to connect these local connectomes into tracks to reveal the subcomponent of fascicles that express associations. (c) The connectometry results can be statistically tested by a permutation test. The permuted (upper row) and non-permuted (lower row) local connectome matrices are associated with body mass index (BMI). Local connectomes that express negative associations with BMI are shown by colored sticks (blue: permuted red: non-permuted). These local connectomes can then be connected into "tracks" using a tracking algorithm to reveal the subcomponents of the fiber pathways that have negative associations. The non-permuted condition identifies several fiber pathways associated with BMI, whereas permuted local connectome matrix generates fragments of pathways. A simple length threshold can be applied to differentiate true and false findings. The false discovery rate can be calculated by the ratio of track count between non-permuted and permuted condition. (d) In 59-subject data set from CMU, the length histogram of tracks that express negative associations (non-permuted) is compared with the null distribution (permuted). The large discrepancy between two histogram curves suggests that there are tracks with a substantial decrease of local connectome due to BMI. The area ratio under two curves is false discovery rate of the findings. The same analysis is applied to study positive association with BMI. The length histogram shows substantial similarity between permuted and non-permuted conditions, suggesting that the positive associations between local connectome and BMI are no different from random effect. (e) In the 488-subject data set from WU-Min HCP, the length histogram of tracks that express negative associations (non-permuted) is compared with the null distribution (permuted). There is a large discrepancy between permuted and non-permuted conditions, suggesting a negative association with BMI. The positive associations between local connectome and BMI are no different from random effects.

linear regression model. The false discovery rate of the uncorrected p-values was calculated using MATLAB (MathWorks, Inc.).

Comparison with tractography analysis

We chose the inferior longitudinal fasciculus (ILF) as the analysis targets because it showed significant associations with BMI in the connectometry analysis. The ILF was tracked on the CMU-BU 80 atlas using the same fiber tracking algorithm (Yeh et al., 2013b), and the

QA values (Yeh et al., 2010) along the ILF were correlated with BMI, age, and sex using a linear regression model. The T-score corresponding to BMI were rendered on ILF to examine whether correlation was localized. To test whether the connectivity at ILF was correlated with BMI, the QA values at ILF were averaged for each subject and correlated with BMI, age, and sex using a linear regression model. The scatter plot of average QA values against BMI was generated for comparison, and the p-value of the BMI association was calculated using the regression model.



Data analysis

The source code for connectometry described in this work is publicly available at <https://github.com/frankyeh/DSI-Studio>, and the atlases described in this paper can be downloaded from <http://dsi-studio.labsolver.org>. The data analysis was conducted on a personal laptop equipped with a 4.0 GHz quad-core CPU and 32 GB memory. A total of 8 threads were used in computation. The CMU data (59 subjects, 2-mm resolution) used a total of 1 gigabytes of memory, and the computation time was around 3 min, whereas the HCP data (488 subjects, 1-mm resolution) used a total of 18 GB memory, the computation time was around 3 h.

Results

Local connectome associations

In order to illustrate the analytical potential of local connectomes, we first show how study-relevant patterns can be identified along local white matter fascicles in the CMU sample and follow up with a replication of these findings in the HCP sample. The local connectome matrix from the CMU sample is shown in Fig. 5. This illustrates the large number of features (columns) relative to the number of samples (rows). Local connectome values from the CMU subjects were then regressed against BMI, sex, and age using linear regression. Consistent with previous findings (Gianaros et al., 2013; Mueller et al., 2011; Stanek et al., 2011; Verstynen et al., 2013, Verstynen et al., 2012), we found many local connectomes that expressed a negative association (i.e., decreased in local connectome as BMI increased) (Fig. 6a). These local connectomes, termed negatively associated local connectomes, appear to be distributed coherently along fiber bundles, supporting the core hypothesis that patterns of variability tend to propagate along a common fiber pathway. The negatively associated local connectomes were then tracked using a fiber tracking algorithm, and the tracking was restricted only to local connectome with substantial associations determined by the Otsu's threshold, so as to reveal the sub-components of fascicles that have negative associations with BMI (Fig. 6b). The negative BMI associations are broadly distributed across white matter pathways in a largely bilateral pattern. This result is consistent with a previous study showing BMI's heterogeneous association to white matter pathways across the brain (see Verstynen et al., 2013).

After identifying study-relevant associations, our next task was to assess the statistical significance of these associations and to correct for multiple comparisons. To do this we applied random permutations to the row vectors of the local connectome matrix and recalculated its association with BMI in order to visualize the null distribution of the negatively associated local connectomes. As shown in the upper row of Fig. 6c, these "null" local connectomes tend to be randomly distributed within white matter, and tracks connected from them are short-distanced fragments that suggest poor continuity along the core fiber pathways. This is substantially different from the non-permuted condition (lower row of Fig. 6c), where the negatively associated local connectomes produce longer tracks. By repeating the random permutations 5000 times we can obtain a null distribution of track lengths if associations to BMI were determined by chance. The true findings and false findings can then be differentiated using a simple length threshold, and the false discovery rate (FDR) can be directly calculated from the length histogram obtained from permuted and non-permuted conditions. These length histograms allows for identifying the length threshold that yields tracks with significant association ($FDR < 0.05$).

To illustrate this, we calculated the length histograms for both positive and negative local connectome associations with BMI using the CMU data set (Fig. 6d). The length histograms of negative associations (local connectomes decrease as BMI increases) show substantial differences between the permuted and non-permuted distributions. Lengths longer than 52, 42, and 31 mm correspond to FDRs of 0.05, 0.075, and

0.10, respectively. By contrast, the length histograms of positive associations (local connectomes increase as BMI increases) show substantial overlap between permuted and non-permuted distributions, suggesting that the positive association between local connectome and BMI cannot be distinguished from random chance. We applied the same connectometry analysis for BMI-associations in the 488 subjects in the HCP sample. As with the CMU sample, the negative associations with BMI were more frequent in the HCP sample than the positive associations. For the negatively associated local connectomes, lengths longer than 14 mm correspond to an FDR of 0.05 (Fig. 6e), showing that a large sample and a higher spatial resolution may increase the statistical power of connectometry to detect finer structural associations.

Since statistical power varies with sample size, the FDR threshold can be used to adjust the sensitivity and specificity of the connectometry analysis when working with lower powered data. Using the CMU data set as an example, a high FDR affords better sensitivity for exploratory analysis, but it also increases false positive rates (e.g. $FDR < 0.1$ in Fig. 7a). A lower FDR offers a more specific result for confirmation of the change in white matter structure; however, the results may miss minor branches and has false negative results (e.g. $FDR < 0.05$ in Fig. 7a). Thus, the FDR adjustment offers the flexibility for different research purposes (e.g. exploratory or confirmative) by either controlling to a predefined threshold (e.g., 0.05) or using a predefined length threshold (e.g., >40 mm) and returning the FDR at that threshold. The FDR values can be affected by the image quality and the number of subjects included in the analysis. Using the HCP data set as an example, we show that with a larger subject pool and a higher spatial resolution, we may capture the associations in short-ranged connections as $FDR < 0.05$ corresponds to lengths longer than 14 mm (Fig. 7b).

Comparison with conventional diffusion MRI analyses

To illustrate how connectometry may complement conventional approaches, we applied variants of conventional end-to-end connectivity at gray matter targets (Hagmann et al., 2008, 2010a, 2010b). The connectivity matrices of the CMU subjects were created using Automated Anatomical Labeling (AAL) atlas for cortical parcellation and the mean quantitative anisotropic (QA) value along the connecting trajectories as the matrix entry. The connectivity matrices were regressed against BMI, age, and sex using linear regression to produce a new matrix of pairwise BMI-associations. Although the BMI-related coefficient matrix in Fig. 8a shows no obvious correlation trend pattern between BMI and the connectivity, the matrix has 79.52% of its non-zero entries being negative, suggesting an overall negative correlation between BMI and QA that is consistent with our connectometry results. The uncorrected p-value map (Fig. 8b), in general, shows a greater significance level at the intra-hemispheric connections (near the diagonal elements). However, the FDR of the most significant p-values is 0.1817, and an alpha threshold of 0.05 will yield no significant pairwise associations in the entire matrix, meaning that typical adjustments for multiple comparisons would wipe out any BMI associations on end-to-end connectivity. Nonetheless, the fact that BMI associates with individual pairwise connections suggests that topological properties of the matrix (e.g., associativity, centrality) also vary with BMI. This pattern of end-to-end connectivity variation is consistent with the distributed pathways identified in the connectometry analysis, suggesting that connectometry provides complementary details about which sub-components of connections within the fascicle are significantly associated with BMI.

We also compared our connectometry results to typical tractography-based region of interest analysis. The inferior longitudinal fasciculus (ILF) was mapped using the CMU/BU 80 atlas, and the mean QA values along ILF were regressed with BMI, age, and sex. The ILF was chosen for illustrative purposes only due to its significant negative BMI associations in the connectometry analysis. The BMI-associated

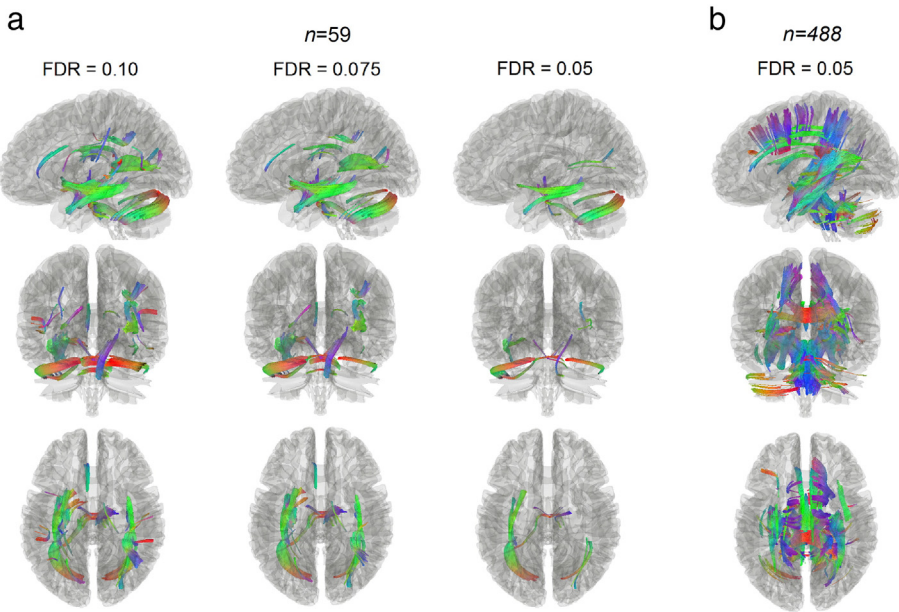


Fig. 7. Impact of FDR threshold and sample size on connectometry results. (a) The subjects from the CMU data set are analyzed by connectometry to reveal the subcomponents of fascicles that express negative associations with BMI. The false discovery rate (FDR) can be controlled to change the sensitivity and specificity of the findings. High FDR leads to more specific results but may miss true findings, while low FDR is more sensitive but may include false positive findings. (b) The HCP sample was analyzed by connectometry to reveal the subcomponents of fascicles that express negative associations with BMI. Inclusion of more study subjects allow for revealing smaller branches of fascicles that achieve significant associations.

t-statistics are rendered to the track bundle (Fig. 8c) in order to illustrate the degree of associations along the entire pathway. The anterior region of the ILF shows the strongest negative association with BMI, whereas the posterior segment shows weaker associations. This suggests that, within the region of interest, the magnitude of BMI associations varies substantially, making averaging across the ROI a conservative estimate of BMI–white matter associations. This is captured in the scatter plot in Fig. 8d, showing a negative association between BMI and the mean QA sampled across the entire ILF. As expected the relationship between BMI and mean QA is strong but not statistically significant ($p = 0.06$). Thus, in this case, region-of-interest analysis is not sensitive enough to reveal the focal effect of BMI because it collapses across the entire fascicle and fails to consider regional variation in BMI associations within the pathway, whereas connectometry naturally isolates only the affected segment of the fascicle, thus achieving greater statistical sensitivity.

Discussion

Here we illustrate the analytical advantage of using the local connectome to identify white matter fascicles that express significant

study-related patterns of variability. While conventional connectome analyses are designed to find differences in whole fiber pathways, connectometry tracks the differences along the pathways themselves. Using data from two independent samples of subjects, scanned using different diffusion MRI approaches, we were able to identify subcomponents of many major white matter pathways associated with BMI. This also suggested that we can track statistically meaningful associations to identify subcomponents of white matter pathways associated with a particular variable of interest. We also show how the spatial specificity of connectometry can complement conventional end-to-end structural connectivity approaches (Hagmann et al., 2008; Rubinov and Sporns, 2010; Sporns et al., 2005). While the full connectivity matrix estimated from diffusion MRI tractography between gray matter targets catches large-scale associations at a network level, connectometry characterizes focal structural differences within the connected pathways that may drive any observed changes in connectivity. On the other hand, connectometry can be viewed as an alternative to conventional tractography-based region-of-interest analyses that aim to identify tracks first and then conduct analysis of anisotropy and diffusivity associated within the identified trajectories (Abhinav et al., 2014b; Jbabdi

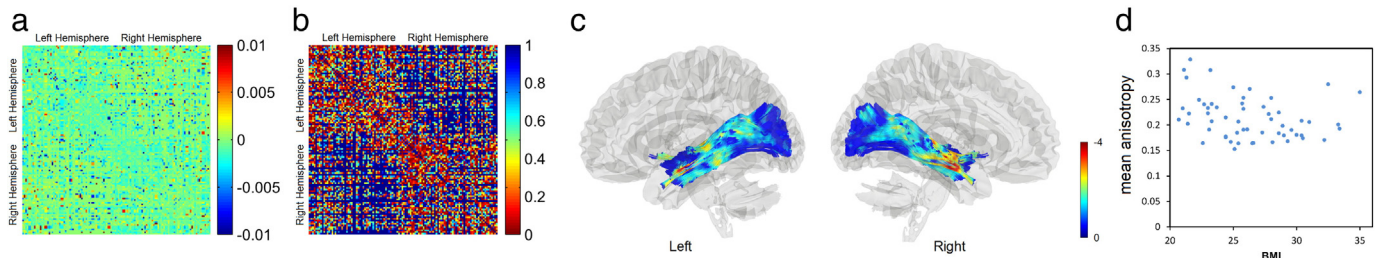


Fig. 8. Conventional connectome analysis applied to study BMI effect on white matter tracks. (a) The BMI-related coefficient matrix has 79.52% of its non-zero entries being negative, suggesting an overall trend of negative correlation between BMI and the connectivity. (b) The uncorrected p-value map shows that the intra-hemisphere connections have a greater significance level. (c) The t-statistics of BMI-related coefficients rendered on inferior longitudinal fasciculus show a focal effect of BMI on the fiber pathways. The structural change involves only a subcomponent of the entire fiber pathways. This suggests that the local connectome is a more suitable measurement to study the BMI effect on track integrity. (d) The scatter plot shows the mean anisotropy values of the fiber pathways against BMI. A linear regression model including age and sex is used to examine the correlation between the mean anisotropy value and BMI. The correlation is not significant ($p\text{-value} = 0.06$). This demonstrates that tractography-based analysis is not power enough if the structure change involves only a segment of the fiber pathway.

and Johansen-Berg, 2011). The tractography-based analysis produces a more conservative estimate of white matter associations that sometimes inflates Type II error rates by averaging across many white matter voxels that may not have strong associations with the study variable of interest. By contrast, connectometry does not map the connectome itself. It analyzes difference in local connectome, associates local connectome with study variables, and then tracks the associations across a pathway. It is able to capture focal structural patterns in a sub-component of individual white matter fascicles, rather than the entire pathway itself. This provides a measure that is highly sensitive to regional variability in white matter and that can complement or inform graph-based connectomic analyses on the end-to-end connections.

Most diffusion MRI connectomics are conducted in a native subject space due to the methodological challenges in warping diffusion information to the stereotaxic space (Hagmann et al., 2010a, Hagmann et al., 2008, Hagmann et al., 2007, Hagmann et al., 2010b; Sporns et al., 2005). Connectometry bridges this gap by using q-space diffeomorphic reconstruction to reconstruct data directly in the stereotaxic space, allowing for integrating voxel-wise diffusion models (e.g., SDFs) across subjects and data sets (e.g. different diffusion schemes). This approach also allows for greater integration of structural analyses with functional imaging data analyzed in MNI-space, even in cases where fMRI data are collected on separate groups of subjects, opening the door to studying generalized structure–function relationships across studies.

Another advantage of connectometry is the atlas-based analysis in a standardized stereotaxic space. While atlas-based analysis has been the norm in fMRI for nearly two decades, there are only few studies using an atlas to analyze diffusion MRI measurements. Tract-based spatial statistics (TBSS) (Smith et al., 2006) uses a “skeleton” to analyze fractional anisotropy (FA), a diffusion index derived from a tensor model. The FA measure has been shown to reflect components of fiber integrity (Huisman et al., 2004; Werring et al., 2000), but studies have also shown that FA is susceptible to the partial volume of crossing fibers (Alexander et al., 2001, Alexander et al., 2002; Ouchi et al., 2007; Tuch et al., 2002; Yendiki et al., 2013). A more recent study used a fiber orientation distribution (FOD) template to analyze streamline count at each fiber direction (Raffelt et al., 2015), but whether stream count can be reliably correlated with the underlying anatomy has been put under question (Besseling et al., 2012; Jbabdi and Johansen-Berg, 2011; Jones et al., 2013). In comparison, connectometry uses the density of diffusion spins derived from a model free approach as the core diffusion measurement to reveal the compactness of fiber bundles (Yeh and Tseng, 2011; Yeh et al., 2013b). The density measurement is consistent across different diffusion schemes (Yeh and Tseng, 2013; Yeh et al., 2010, 2011), thus allowing connectometry to be applied to a variety of acquisition approaches, including conventional DTI, multi-shell diffusion images, and DSI. This feature is critical for comparing results across multiple studies and/or test sites. Connectometry also adopts a new paradigm—tracking the difference—to investigate the association of the diffusion measurement with a study variable. This paradigm is different from the conventional paradigm that seeks to map cortical connections (i.e. end-to-end connections) first and then study their associations. Mapping end-to-end connections has been a challenge due to methodological limitations (Jones et al., 2013; Reveley et al., 2015; Thomas et al., 2014), and a reliable and reproducible approach is still under active research. Connectometry bypasses this limitation by first quantifying the local associations and tracking only a subcomponent of the fiber pathway that expresses substantial association. The length of the affected subcomponent is used as the statistical index to help differentiate true findings from false findings caused by misalignment. Connectometry is also highly extensible to most regression frameworks due to the *independent and identically distributed* (i.i.d.) feature of the local connectome matrix. The ordinary least squares regression model used here can be replaced by sparse or non-linear regression approaches for more precise results. Also, non-regression metrics such as

group mean difference, paired difference, or percentile rank test can also be used to estimate the first state associations (Fig. 2b). Using different models, connectometry can examine associations between two groups of subjects, or to examine the change before and after a treatment, or to compare the connectivity differences between an individual with a normal population. Having a well characterized distribution of healthy normal variability in the normal local connectome could allow connectometry to be used to identify the white matter areas with pathological differences in clinical patients with neurological, psychological, and psychiatric disorders, providing a quantifiable and potential biomarker for white matter pathologies. While the initial concept of connectometry was proposed as a way of identifying pathological damage by comparing individuals with neurological damage to a normal population (Abhinav et al., 2014a, Abhinav et al., 2014b; Yeh et al., 2013a), here we extend the approach to include a regression model as a more general framework for group-wise, atlas-based comparison. This enables us to study the effect of BMI while also considering age and sex as the confounding factors. The extension can be applied to a large scale study that includes a complex set of demographic information to study the association between brain structure and a study variable.

In conclusion, we show how analyzing local connectomic patterns can be a powerful method for investigating variability in macroscopic white matter pathways. Connectometry can serve as a complementary approach for conventional structural connectomics. In the future, connectometry may further open the door to applying more sophisticated statistical models, such as machine learning classifiers, to investigate how brain structure associates with a study variable and highlights a rich clinical potential connectometry as a classifier for clinical pathologies.

Acknowledgments

Data were provided in part by the Human Connectome Project, WU-Minn Consortium (D. Van Essen and K. Ugurbil, 1U54MH091657 NIH). This research was sponsored by the Army Research Laboratory and was accomplished under Cooperative Agreement Number W911NF-10-2-0022. The views and conclusions contained in this document are those of the authors and should not be interpreted as representing the official policies, either expressed or implied, of the Army Research Laboratory or the U.S. Government. The U.S. Government is authorized to reproduce and distribute reprints for Government purposes notwithstanding any copyright notation herein. This research was supported by an NSF BIGDATA Grant #1247658.

References

- Abhinav, K., Yeh, F.C., El-Dokla, A., Ferrando, L.M., Chang, Y.F., Lacomis, D., Friedlander, R.M., Fernandez-Miranda, J.C., 2014a. Use of diffusion spectrum imaging in preliminary longitudinal evaluation of amyotrophic lateral sclerosis: development of an imaging biomarker. *Front. Hum. Neurosci.* 8, 270.
- Abhinav, K., Yeh, F.C., Pathak, S., Suski, V., Lacomis, D., Friedlander, R.M., Fernandez-Miranda, J.C., 2014b. Advanced diffusion MRI fiber tracking in neurosurgical and neurodegenerative disorders and neuroanatomical studies: a review. *Biochim. Biophys. Acta* 1842, 2286–2297.
- Akil, H., Martone, M.E., Van Essen, D.C., 2011. Challenges and opportunities in mining neuroscience data. *Science* 331, 708–712.
- Alexander, A.L., Hasan, K.M., Lazar, M., Tsuruda, J.S., Parker, D.L., 2001. Analysis of partial volume effects in diffusion-tensor MRI. *Magn. Reson. Med.* 45, 770–780.
- Alexander, D.C., Barker, G.J., Arridge, S.R., 2002. Detection and modeling of non-Gaussian apparent diffusion coefficient profiles in human brain data. *Magn. Reson. Med.* 48, 331–340.
- Ashburner, J., Friston, K.J., 1999. Nonlinear spatial normalization using basis functions. *Hum. Brain Mapp.* 7, 254–266.
- Besseling, R.M., Jansen, J.F., Overvliet, G.M., Vaessen, M.J., Braakman, H.M., Hofman, P.A., Aldenkamp, A.P., Backes, W.H., 2012. Tract specific reproducibility of tractography based morphology and diffusion metrics. *PLoS One* 7, e34125.
- Biswal, B.B., Mennies, M., Zuo, X.N., Cohen, S., Kelly, C., Smith, S.M., Beckmann, C.F., Adelstein, J.S., Buckner, R.L., Colcombe, S., Dogonowski, A.M., Ernst, M., Fair, D., Hampson, M., Hoptman, M.J., Hyde, J.S., Kiviniemi, V.J., Kotter, R., Li, S.J., Lin, C.P., Lowe, M.J., Mackay, C., Madden, D.J., Madsen, K.H., Margulies, D.S., Mayberg, H.S., McMahon, K., Monk, C.S., Mostofsky, S.H., Nagel, B.J., Pekar, J.J., Peltier, S.J., Petersen,

- S.E., Riedl, V., Rombouts, S.A., Rypma, B., Schlaggar, B.L., Schmidt, S., Seidler, R.D., Siegle, G.J., Sorg, C., Teng, G.J., Veijola, J., Villringer, A., Walter, M., Wang, L., Weng, X.C., Whitfield-Gabrieli, S., Williamson, P., Windischberger, C., Zang, Y.F., Zhang, H.Y., Castellanos, F.X., Milham, M.P., 2010. Toward discovery science of human brain function. *Proc. Natl. Acad. Sci. U. S. A.* 107, 4734–4739.
- Bullmore, E., Sporns, O., 2009. Complex brain networks: graph theoretical analysis of structural and functional systems. *Nat. Rev. Neurosci.* 10, 186–198.
- Craddock, R.C., Jbabdi, S., Yan, C.G., Vogelstein, J.T., Castellanos, F.X., Di Martino, A., Kelly, C., Heberlein, K., Colcombe, S., Milham, M.P., 2013. Imaging human connectomes at the macroscale. *Nat. Methods* 10, 524–539.
- Defelipe, J., 2010. From the connectome to the synaptome: an epic love story. *Science* 330, 1198–1201.
- Dolgin, E., 2010. This is your brain online: the Functional Connectomes Project. *Nat. Med.* 16, 351.
- Fornito, A., Zalesky, A., Breakspear, M., 2015. The connectomics of brain disorders. *Nat. Rev. Neurosci.* 16, 159–172.
- Gianaros, P.J., Marsland, A.L., Sheu, L.K., Erickson, K.I., Verstynen, T.D., 2013. Inflammatory pathways link socioeconomic inequalities to white matter architecture. *Cereb. Cortex* 23, 2058–2071.
- Hagmann, P., Kurant, M., Gigandet, X., Thiran, P., Wedeen, V.J., Meuli, R., Thiran, J.P., 2007. Mapping human whole-brain structural networks with diffusion MRI. *PLoS One* 2, e597.
- Hagmann, P., Cammoun, L., Gigandet, X., Meuli, R., Honey, C.J., Wedeen, V.J., Sporns, O., 2008. Mapping the structural core of human cerebral cortex. *PLoS Biol.* 6, e159.
- Hagmann, P., Cammoun, L., Gigandet, X., Gerhard, S., Grant, P.E., Wedeen, V., Meuli, R., Thiran, J.P., Honey, C.J., Sporns, O., 2010a. MR connectomics: principles and challenges. *J. Neurosci. Methods* 194, 34–45.
- Hagmann, P., Sporns, O., Madan, N., Cammoun, L., Pienaar, R., Wedeen, V.J., Meuli, R., Thiran, J.P., Grant, P.E., 2010b. White matter maturation reshapes structural connectivity in the late developing human brain. *Proc. Natl. Acad. Sci. U. S. A.* 107, 19067–19072.
- Honey, C.J., Sporns, O., Cammoun, L., Gigandet, X., Thiran, J.P., Meuli, R., Hagmann, P., 2009. Predicting human resting-state functional connectivity from structural connectivity. *Proc. Natl. Acad. Sci. U. S. A.* 106, 2035–2040.
- Huisman, T.A., Schwamm, L.H., Schaefer, P.W., Koroshetz, W.J., Shetty-Alva, N., Ozsunar, Y., Wu, O., Sorenson, A.G., 2004. Diffusion tensor imaging as potential biomarker of white matter injury in diffuse axonal injury. *AJNR Am. J. Neuroradiol.* 25, 370–376.
- Jbabdi, S., Johansen-Berg, H., 2011. Tractography: where do we go from here? *Brain Connect.* 1, 169–183.
- Johansen-Berg, H., Behrens, T.E., Robson, M.D., Drobniak, I., Rushworth, M.F., Brady, J.M., Smith, S.M., Higham, D.J., Matthews, P.M., 2004. Changes in connectivity profiles define functionally distinct regions in human medial frontal cortex. *Proc. Natl. Acad. Sci. U. S. A.* 101, 13335–13340.
- Jones, D.K., Knosche, T.R., Turner, R., 2013. White matter integrity, fiber count, and other fallacies: the do's and don'ts of diffusion MRI. *NeuroImage* 73, 239–254.
- Mueller, K., Anwander, A., Moller, H.E., Horstmann, A., Lepsién, J., Busse, F., Mohammadi, S., Schroeter, M.L., Stumvoll, M., Villringer, A., Pleger, B., 2011. Sex-dependent influences of obesity on cerebral white matter investigated by diffusion-tensor imaging. *PLoS One* 6, e18544.
- Nichols, T.E., Holmes, A.P., 2002. Nonparametric permutation tests for functional neuroimaging: a primer with examples. *Hum. Brain Mapp.* 15, 1–25.
- Oouchi, H., Yamada, K., Sakai, K., Kizu, O., Kubota, T., Ito, H., Nishimura, T., 2007. Diffusion anisotropy measurement of brain white matter is affected by voxel size: underestimation occurs in areas with crossing fibers. *AJNR Am. J. Neuroradiol.* 28, 1102–1106.
- Otsu, N., 1979. A threshold selection method from gray-level histograms. *IEEE Trans. Syst. Man Cybern.* 9, 62–66.
- Pestilli, F., Yeatman, J.D., Rokem, A., Kay, K.N., Wandell, B.A., 2014. Evaluation and statistical inference for human connectomes. *Nat. Methods* 11, 1058–1063.
- Raffelt, D.A., Smith, R.E., Ridgway, G.R., Tournier, J.D., Vaughan, D.N., Rose, S., Henderson, R., Connelly, A., 2015. Connectivity-based fixel enhancement: whole-brain statistical analysis of diffusion MRI measures in the presence of crossing fibres. *NeuroImage* 117, 40–55.
- Reveley, C., Seth, A.K., Pierpaoli, C., Silva, A.C., Yu, D., Saunders, R.C., Leopold, D.A., Ye, F.Q., 2015. Superficial white matter fiber systems impede detection of long-range cortical connections in diffusion MR tractography. *Proc. Natl. Acad. Sci. U. S. A.* 112, E2820–E2828.
- Rubinov, M., Sporns, O., 2010. Complex network measures of brain connectivity: uses and interpretations. *NeuroImage* 52, 1059–1069.
- Seung, H.S., 2011. Neuroscience: towards functional connectomics. *Nature* 471, 170–172.
- Smith, S.M., Jenkinson, M., Johansen-Berg, H., Rueckert, D., Nichols, T.E., Mackay, C.E., Watkins, K.E., Ciccarelli, O., Cader, M.Z., Matthews, P.M., Behrens, T.E., 2006. Tract-based spatial statistics: voxelwise analysis of multi-subject diffusion data. *NeuroImage* 31, 1487–1505.
- Sotiropoulos, S.N., Jbabdi, S., Xu, J., Andersson, J.L., Moeller, S., Auerbach, E.J., Glasser, M.F., Hernandez, M., Sapiro, G., Jenkinson, M., Feinberg, D.A., Yacoub, E., Lenglet, C., Van Essen, D.C., Ugurbil, K., Behrens, T.E., 2013. Advances in diffusion MRI acquisition and processing in the Human Connectome Project. *NeuroImage* 80, 125–143.
- Sporns, O., 2013. The human connectome: origins and challenges. *NeuroImage* 80, 53–61.
- Sporns, O., 2014a. Contributions and challenges for network models in cognitive neuroscience. *Nat. Neurosci.* 17, 652–660.
- Sporns, O., 2014b. Towards network substrates of brain disorders. *Brain* 137, 2117–2118.
- Sporns, O., Tononi, G., Kotter, R., 2005. The human connectome: a structural description of the human brain. *PLoS Comput. Biol.* 1, e42.
- Stanek, K.M., Grieve, S.M., Brickman, A.M., Korgaonkar, M.S., Paul, R.H., Cohen, R.A., Gunstad, J.J., 2011. Obesity is associated with reduced white matter integrity in otherwise healthy adults. *Obesity (Silver Spring)* 19, 500–504.
- Thomas, C., Ye, F.Q., Irfanoglu, M.O., Modi, P., Saleem, K.S., Leopold, D.A., Pierpaoli, C., 2014. Anatomical accuracy of brain connections derived from diffusion MRI tractography is inherently limited. *Proc. Natl. Acad. Sci. U. S. A.* 111, 16574–16579.
- Tuch, D.S., Reese, T.G., Wiegell, M.R., Makris, N., Belliveau, J.W., Wedeen, V.J., 2002. High angular resolution diffusion imaging reveals intravoxel white matter fiber heterogeneity. *Magn. Reson. Med.* 48, 577–582.
- Turk-Browne, N.B., 2013. Functional interactions as big data in the human brain. *Science* 342, 580–584.
- Verstynen, T.D., Weinstein, A.M., Schneider, W.W., Jakicic, J.M., Rofey, D.L., Erickson, K.I., 2012. Increased body mass index is associated with a global and distributed decrease in white matter microstructural integrity. *Psychosom. Med.* 74, 682–690.
- Verstynen, T.D., Weinstein, A., Erickson, K.I., Sheu, L.K., Marsland, A.L., Gianaros, P.J., 2013. Competing physiological pathways link individual differences in weight and abdominal adiposity to white matter microstructure. *NeuroImage* 79, 129–137.
- Wedeen, V.J., Rosene, D.L., Wang, R., Dai, G., Mortazavi, F., Hagmann, P., Kaas, J.H., Tseng, W.Y., 2012. The geometric structure of the brain fiber pathways. *Science* 335, 1628–1634.
- Werring, D.J., Toosy, A.T., Clark, C.A., Parker, G.J., Barker, G.J., Miller, D.H., Thompson, A.J., 2000. Diffusion tensor imaging can detect and quantify corticospinal tract degeneration after stroke. *J. Neurol. Neurosurg. Psychiatry* 69, 269–272.
- Yeh, F.C., Tseng, W.Y., 2011. NTU-90: a high angular resolution brain atlas constructed by q-space diffeomorphic reconstruction. *NeuroImage* 58, 91–99.
- Yeh, F.C., Tseng, W.Y., 2013. Sparse solution of fiber orientation distribution function by diffusion decomposition. *PLoS One* 8, e75747.
- Yeh, F.C., Wedeen, V.J., Tseng, W.Y., 2010. Generalized q-sampling imaging. *IEEE Trans. Med. Imaging* 29, 1626–1635.
- Yeh, F.C., Wedeen, V.J., Tseng, W.Y., 2011. Estimation of fiber orientation and spin density distribution by diffusion deconvolution. *NeuroImage* 55, 1054–1062.
- Yeh, F.C., Tang, P.F., Tseng, W.Y., 2013a. Diffusion MRI connectometry automatically reveals affected fiber pathways in individuals with chronic stroke. *NeuroImage Clin.* 2, 912–921.
- Yeh, F.C., Verstynen, T.D., Wang, Y., Fernandez-Miranda, J.C., Tseng, W.Y., 2013b. Deterministic diffusion fiber tracking improved by quantitative anisotropy. *PLoS One* 8, e80713.
- Yendiki, A., Kolodewyn, K., Kakunoori, S., Kanwisher, N., Fischl, B., 2013. Spurious group differences due to head motion in a diffusion MRI study. *NeuroImage* 88C, 79–90.